

Lattice study on a tetraquark state T_{bb} in the HAL QCD method

Sinya Aoki^{a,b,*} and Takafumi Aoki^c

^aCenter for Gravitational Physics and Quantum Information, Yukawa Institute for Theoretical Physics, Kyoto University, Koto 606-8502, Japan

^bInterdisciplinary Theoretical and Mathematical Sciences Program (iTHEMS), RIKEN, Wako 351-0198, Japan

^cYukawa Institute for Theoretical Physics, Kyoto University, Koto 606-8502, Japan

E-mail: saoki@yukawa.kyoto-u.ac.jp , takafumi.aoki@yukawa.kyoto-u.ac.jp

We investigate a doubly-bottomed tetraquark state T_{bb} ($bb\bar{u}\bar{d}$) with quantum number $I(J^P) = 0(1^+)$ in $(2+1)$ -flavor lattice QCD. Using the Non-Relativistic QCD (NRQCD) quark action for b quarks, we have extracted the coupled channel potential between $\bar{B}\bar{B}^*$ and $\bar{B}^*\bar{B}^*$ in the HAL QCD method at $a \approx 0.09$ fm on $32^3 \times 64$ lattices. The potential predicts an existence of a bound T_{bb} below the $\bar{B}\bar{B}^*$ threshold. At the physical pion mass $m_\pi \approx 140$ MeV extrapolated from $m_\pi \approx 410, 570, 700$ MeV, a binding energy with its statistical error is given by $E_{\text{binding}}^{(\text{coupled})} = 83(10)$ MeV from a coupled channel analysis where effects due to virtual $\bar{B}^*\bar{B}^*$ states are included through the coupled channel potential, while we obtain $E_{\text{binding}}^{(\text{single})} = 155(17)$ MeV only from a potential for a single $\bar{B}\bar{B}^*$ channel. This difference indicates that the effect from virtual $\bar{B}^*\bar{B}^*$ states is sizable to the binding energy of T_{bb} . Adding ± 20 MeV as empirical systematic error caused by the NRQCD approximation for b quarks, our estimate of the T_{bb} binding energy becomes $83(10)(20)$ MeV.

*The 39th International Symposium on Lattice Field Theory (Lattice2022),
8-13 August, 2022
Bonn, Germany*

*Speaker

1. Introduction

A tetraquark state is one of exotic states in QCD other than mesons and baryons and is made of two quarks and two antiquarks. Recently heavy tetraquark states, made of two heavy quarks and two light antiquarks, attract much attentions, probably because they are genuine tetraquark states as $QQ\bar{q}\bar{q}$ or $qq\bar{Q}\bar{Q}$, where Q and q are a heavy and a light quarks respectively. We denote such a heavy tetraquark state as T_{QQ} . Indeed, an observation of T_{cc} ($cc\bar{u}\bar{d}$) state just below the $D^{*+}D^0$ threshold was reported by the LHCb collaboration[1]. While results from previous lattice QCD calculations[2, 3] were inconclusive, the latest lattice QCD study[4] suggests a virtual state for T_{cc} .

Another candidate for heavy tetraquark states is T_{bb} ($bb\bar{u}\bar{d}$ or $\bar{b}\bar{b}ud$), which has not been observed yet but is more likely to exist as a bound state than T_{cc} , since a force between two \bar{b} is probably described by a screened Coulomb potential, generated as a mixture of one-gluon-exchange at short distance and a screening due to light quarks at long distance.

There are several lattice studies on T_{bb} . The single channel potential between \bar{B} and \bar{B}^* , calculated using the static quark action to treat b quarks on the lattice, predicted an existence of one bound state in the $I(J^P) = 0(1^+)$ channel, whose binding energy is extrapolated to the physical pion mass as $E_B = 90_{-36}^{+43}$ [5]. The coupled channel potential between $\bar{B}\bar{B}^*$ and $\bar{B}^*\bar{B}^*$ reduces the binding energy to $E_B = 59_{-38}^{+30}$ [6]. Direct spectrum calculations in lattice QCD using NRQCD for b quarks to include their moving in space increase the binding energy significantly to $E_B \simeq 120 \sim 165$ MeV[7–9].

Aims of our study are to confirm an existence of a bound T_{bb} and to investigate its properties, employing the HAL QCD potential method[10–12], which is different from methods in previous studies. In particular, we have performed a coupled channel analysis with moving b quarks by NRQCD, in order to see how competing effects, the reduction by the coupled channel and the enhancement by the moving b quarks, finally determines the binding energy of T_{bb} .

2. Methodology

2.1 HAL QCD method

Since a threshold of the $\mathcal{B}^* := \bar{B}^*\bar{B}^*$ channel is only about 45 MeV above the $\mathcal{B} := \bar{B}\bar{B}^*$ threshold, we have carried out a coupled channel analysis in our study. Namely, we employ the time-dependent coupled channel HAL QCD method[13, 14] at the leading order (LO) in the derivative expansion, which is summarized as follows. The time-dependent 2×2 coupled channel equation reads

$$\underbrace{\left(\frac{\nabla}{2\mu_\alpha} - \frac{\partial}{\partial t} + \frac{1 + \delta_\alpha^2}{8\mu_\alpha} \frac{\partial^2}{\partial t^2} \right)}_{:=\mathcal{K}^\alpha_\xi} R^\alpha_\xi(\mathbf{r}, t) \simeq \sum_\beta \tilde{\Delta}^{\alpha\beta}(t) \int d^3r' U^{\alpha\beta}(\mathbf{r}, \mathbf{r}') R^\beta_\xi(\mathbf{r}', t) \quad (1)$$

where $\alpha, \beta = 0(\mathcal{B}), 1(\mathcal{B}^*)$, μ_α is a reduced mass of the channel α , and

$$\delta_\alpha := \frac{|m_{\alpha_1} - m_{\alpha_2}|}{m_{\alpha_1} + m_{\alpha_2}}, \quad \tilde{\Delta}^{\alpha\beta}(t) = \sqrt{\frac{Z_{\beta_1} Z_{\beta_2}}{Z_{\alpha_1} Z_{\alpha_2}}} \frac{e^{-(m_{\beta_1} + m_{\beta_2})t}}{e^{-(m_{\alpha_1} + m_{\alpha_2})t}}, \quad (2)$$

with m_{α_i} and Z_{α_i} being mass and Z -factor of the i -th particle in the channel α . Here the normalized correlation function for the source operator \mathcal{J}_ξ^\dagger with $\xi = 0, 1$ and hadron operators H_{α_i} is given by

$$R_\xi^\alpha(\mathbf{r}, t - t_0) = \frac{1}{e^{-(m_{\alpha_1} + m_{\alpha_2})(t - t_0)}} \sum_{\mathbf{x}} \langle 0 | H_{\alpha_1}(\mathbf{x} + \mathbf{r}, t) H_{\alpha_2}(\mathbf{x}, t) \mathcal{J}_\xi^\dagger(t_0) | 0 \rangle. \quad (3)$$

A potential matrix at the LO in the derivative expansion of $U^{\alpha\beta}(\mathbf{r}, \mathbf{r}') = V^{\alpha\beta}(\mathbf{r})\delta^{(3)}(\mathbf{r} - \mathbf{r}')$ is extracted from the above equation as

$$\begin{pmatrix} V^{00}(\mathbf{r}) & \tilde{\Delta}^{(01)}(t)V^{01}(\mathbf{r}) \\ \tilde{\Delta}^{(10)}(t)V^{10}(\mathbf{r}) & V^{11}(\mathbf{r}) \end{pmatrix} = \begin{pmatrix} \mathcal{K}^0_0(\mathbf{r}) & \mathcal{K}^0_1(\mathbf{r}) \\ \mathcal{K}^1_0(\mathbf{r}) & \mathcal{K}^1_1(\mathbf{r}) \end{pmatrix} \begin{pmatrix} R^0_0(\mathbf{r}) & R^0_1(\mathbf{r}) \\ R^1_0(\mathbf{r}) & R^1_1(\mathbf{r}) \end{pmatrix}^{-1}. \quad (4)$$

A mild t dependence of the LO potential matrix extracted in the above procedure indicates that inelastic contributions as well as truncation errors in the LO approximation are small.

2.2 NRQCD action for heavy quarks

Since b quarks are too heavy to treat relativistically at lattice spacings in currently available gauge configurations, we have employed the NonRelativistic QCD (NRQCD) formulation[15] for b quarks, where a time evolution of the two-spinor NRQCD propagator G_ψ is controlled by the Hamiltonian $\mathcal{H}_\psi := \mathcal{H}_0 + \delta\mathcal{H}$ as

$$G(\mathbf{x}, t + 1 | s_0) = \left(1 - \frac{\mathcal{H}_0}{2n}\right)^n \left(1 - \frac{\delta\mathcal{H}}{2}\right) U_4^\dagger(x) \left(1 - \frac{\delta\mathcal{H}}{2}\right) \left(1 - \frac{\mathcal{H}_0}{2n}\right)^n G(\mathbf{x}, t | s_0) + s_0(\mathbf{x})\delta_{t,-1}, \quad (5)$$

where $\mathcal{H}_0 = -\frac{1}{2M}\Delta^{(2)}$ is the leading Hamiltonian at $O(v^2)$ with M and v being a mass and a velocity of a b quark, respectively, s_0 is a source vector, and $n = 2$ is a stabilized parameter. In our study, we take $O(v^4)$ terms for $\delta\mathcal{H} = \sum_{i=1}^6 c_i \delta\mathcal{H}^{(i)}$ with

$$\begin{aligned} \delta\mathcal{H}^{(1)} &= -\frac{1}{2M}\boldsymbol{\sigma} \cdot \mathbf{B}, \quad \delta\mathcal{H}^{(2)} = \frac{i}{8M^2}(\nabla \cdot \mathbf{E} - \mathbf{E} \cdot \nabla), \quad \delta\mathcal{H}^{(3)} = -\frac{1}{8M}\boldsymbol{\sigma} \cdot (\nabla \times \mathbf{E} - \mathbf{E} \times \nabla), \\ \delta\mathcal{H}^{(4)} &= -\frac{1}{8M^3}(\Delta^{(2)})^2, \quad \delta\mathcal{H}^{(5)} = \frac{1}{24M}\Delta^{(4)}, \quad \delta\mathcal{H}^{(6)} = -\frac{1}{16nM^2}(\Delta^{(2)})^2, \end{aligned} \quad (6)$$

where all c_i 's are taken to be tree level values ($c_i = 1$) with the tadpole improvement that $U_\mu \rightarrow U_\mu/u_0$ [16], ∇ , $\Delta^{(2)}$, $\Delta^{(2)}$ are 1st, 2nd and 4th order symmetric covariant difference in space, respectively, and the chromo-electromagnetic fields \mathbf{E} and \mathbf{B} are given by the standard clover-leaf definition. Correspondingly, the FWT transformation matrix at $O(v^4)$ [17] is employed in our study.

A mass of heavy-light meson X with the NRQCD b quark is extracted as

$$M_X = \frac{\mathbf{p}^2 - (E_X(\mathbf{p}) - E_X(\mathbf{0}))^2}{2(E_X(\mathbf{p}) - E_X(\mathbf{0}))}, \quad (7)$$

where $E_X(\mathbf{p}) = \sqrt{\mathbf{p}^2 + M_X^2} - \delta$ is an energy of the X meson with a momentum \mathbf{p} , and δ is an additive mass renormalization for the b quark. We do not have to know δ in the above formula.

2.3 Operators

For the coupled channel analysis ($\alpha = 0, 1$), we employ 2 types of meson-meson local sink operators given by

$$\begin{aligned} \mathcal{B}_j(\mathbf{r}) &:= \sum_{\mathbf{x}} \left\{ B_u(\mathbf{x} + \mathbf{r}) B_{d,j}^*(\mathbf{x}) - [u \leftrightarrow d] \right\}, \quad B_q(\mathbf{x}) := \bar{q}(\mathbf{x}) \gamma_5 b(\mathbf{x}), \quad B_{q,j}^*(\mathbf{x}) := \bar{q}(\mathbf{x}) \gamma_j b(\mathbf{x}), \\ \mathcal{B}_j^*(\mathbf{r}) &:= \epsilon_{jkl} \sum_{\mathbf{x}} \left\{ B_{u,k}^*(\mathbf{x} + \mathbf{r}) B_{d,\ell}^*(\mathbf{x}) - [u \leftrightarrow d] \right\}. \end{aligned} \quad (8)$$

Since both \mathcal{B}_j^\dagger and $(\mathcal{B}_j^*)^\dagger$ source operators create similar combinations of two independent states, we introduce a diquark operator made of heavy and light quarks as

$$\mathcal{J}_{\mathcal{D}_j^\dagger} = \left(\epsilon^{abc} \bar{b}^b \gamma_j C \bar{b}^c \right) \left(\epsilon^{ade} \bar{d}^d C \gamma_5 \bar{u}^e \right) - [u \leftrightarrow d], \quad (9)$$

where $C = \gamma_4 \gamma_2$ is a charge-conjugation matrix. To create two different R^α_ξ 's ($\xi = 0, 1$) with wall quark sources in the Coulomb gauge fixing, we take a meson-meson operator $\mathcal{J}_{\mathcal{B}_j^\dagger}$ made of the creation operator of \mathcal{B}_j for $\xi = 0$ and a diquark operator $\mathcal{J}_{\mathcal{D}_j^\dagger}$ for $\xi = 1$.

2.4 Lattice QCD configurations

In our study, we have employed 2 + 1 flavor full QCD configurations generated by the CP-PACS Collaboration[18] with the Iwasaki gauge action and the Wilson-Clover light quark action at $a \simeq 0.09$ fm, and 400 configurations are used at each pion mass, $m_\pi = 701, 571, 461$ MeV. We tune the b quark mass M_b to reproduce the spin-averaged $b\bar{b}$ mass, $M_{b\bar{b}}^{\text{spin-avg.}} \simeq 9450$ MeV, leading to $M_{\bar{B}}^{\text{spin-avg.}} := (M_{\bar{B}} + 3M_{B^*})/4 = 5440(174), 5382(269),$ and $5332(220)$ MeV at each pion mass, which agree with an experimental value, 5313 MeV within 5% statistical errors, while the spin-splitting $\Delta E_{\bar{B}B^*} := M_{B^*} - M_{\bar{B}}$ decreases as 49.4(2.6), 44.9(1.6) and 42.7(3.9) MeV.

3. Numerical results

3.1 Leading order potentials

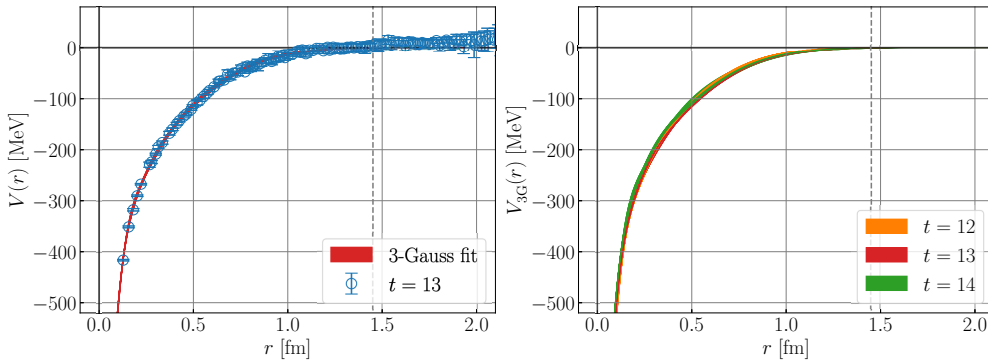


Figure 1: (Left) A single channel potential (blue circles) extracted at $t = 13$, together with the 3 Gaussian fit by a red line. (Right) A comparison among fits at $t = 12, 13, 14$.

Fig. 1 (Left) shows that a potential for a single \mathcal{B} channel is attractive at all distances smaller than 1.0 fm and is well described by a sum of 3 Gaussians (red line). A small t dependence of the potential in Fig. 1 (Right) suggests that contributions from inelastic states as well as higher order terms in the derivative expansion are well under control.

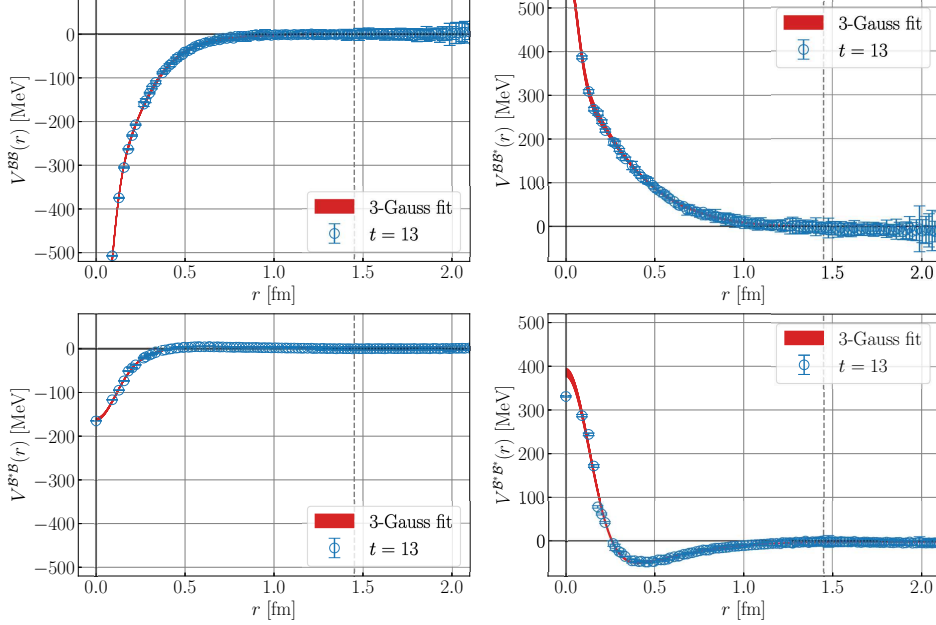


Figure 2: 2×2 coupled-channel potentials (blue circles) extracted at $t = 13$, together with 3 Gaussian fits by red lines.

Fig. 2 shows a LO coupled channel potential at $m_\pi = 701$ MeV, extracted at $t = 13$. A diagonal potential $V^{\mathcal{B}\mathcal{B}}$ is attractive at all distances smaller than 0.8 fm but the range of attraction is shorter than 1.0 fm in the single channel, while $V^{\mathcal{B}^*\mathcal{B}^*}$ has a repulsive core surrounded by an attractive pocket at $r \simeq 0.4$ fm. We have surprisingly found that off-diagonal parts are not symmetric leading to a large violation of the Hermiticity. In addition, off-diagonal interaction between \mathcal{B} and \mathcal{B}^* are comparable to diagonal ones in magnitudes. Therefore, such strong off-diagonal interactions should be taken into account in the scattering analysis even for the single channel scattering below the \mathcal{B}^* threshold, as will be seen in the next subsection.

The coupled channel potential is also well fitted by a sum of 3 Gaussian functions (red lines in Fig. 2) at each pion mass. As the pion mass decreases, both diagonal and off-diagonal potentials become stronger and more long-ranged. Thus a mixing effect due to off-diagonal potentials remains relevant even at the physical pion mass.

3.2 Scattering analysis

Since the Hermiticity of the coupled channel potential is badly violated, probably due to the LO approximation, we consider a single channel scattering in the \mathcal{B} channel below the \mathcal{B}^* threshold while employing 2×2 coupled channel potential V^{XY} to include virtual \mathcal{B}^* states. Integrating

out virtual \mathcal{B}^* contributions, an effective single channel potential becomes non-local and energy-dependent as

$$U_{\text{eff},E}^{\mathcal{B}\mathcal{B}}(\mathbf{x}, \mathbf{y}) = V^{\mathcal{B}\mathcal{B}}(\mathbf{x})\delta^{(3)}(\mathbf{x} - \mathbf{y}) + V^{\mathcal{B}\mathcal{B}^*}(\mathbf{x})G_E^{\mathcal{B}^*\mathcal{B}^*}(\mathbf{x}, \mathbf{y})V^{\mathcal{B}^*\mathcal{B}}(\mathbf{y}), \quad (10)$$

where $G_E^{\mathcal{B}^*\mathcal{B}^*}$ is a propagator of \mathcal{B}^* in the presence of the diagonal potential $V^{\mathcal{B}^*\mathcal{B}^*}$ at energy E .

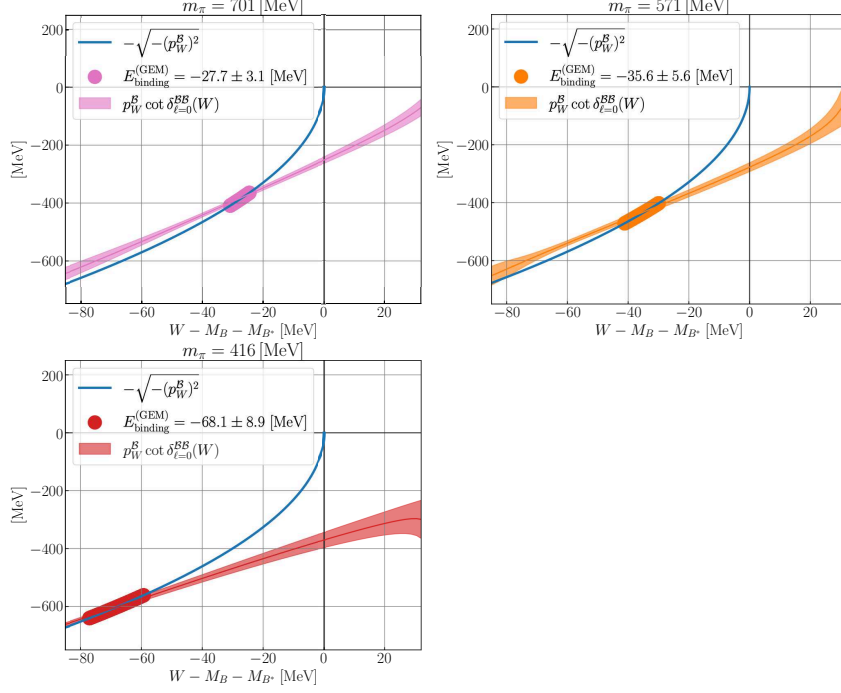


Figure 3: Results of $p \cot \delta(p)$ in the \mathcal{B} channel as a function of the energy measured from the \mathcal{B} threshold, $W - M_{\bar{B}} - M_{B^*}$, at $m_\pi = 701$ (pink), 571 (orange), and 416 (red) MeV, together with the bound state condition, $-\sqrt{-p^2}$, by a blue solid curve. A thin band along $-\sqrt{-p^2}$ curve shows a binding energy calculated by the GEM, which agrees well with an intersection between the $p \cot \delta(W)$ and the bound state condition.

Solving the Lippmann-Schwinger equation with the fitted coupled channel potentials, we extract scattering phase shift $\delta(p)$ in the single channel \mathcal{B} below the inelastic threshold of the channel \mathcal{B}^* , where p is a magnitude of momentum extracted from the center of mass energy as $W = \sqrt{p^2 + M_{\bar{B}}^2} + \sqrt{p^2 + M_{B^*}^2}$. Fig. 3 shows $p \cot \delta(p)$ as a function of the energy from the \mathcal{B} threshold, $W - M_{\bar{B}} - M_{B^*}$, at $m_\pi = 701$ (pink), 571 (orange), and 416 (red) MeV. At $0 < W - M_{\bar{B}} - M_{B^*} < M_{B^*} - M_{\bar{B}} \simeq 45$ MeV, phase shifts $\delta(p)$ is physical, while an existence of a bound state is examined by its analytic continuation at $W - M_{\bar{B}} - M_{B^*} < 0$. Since an analytic continuation of the on-shell T -matrix has a pole at $p \cot \delta(p) = ip$, an intersection between $p \cot \delta(p)$ (pink, orange and red bands) and $-\sqrt{-p^2}$ in Fig. 3 corresponds to a bound states in the \mathcal{B} channel, showing that there exists one bound T_{bb} state at each pion mass. Note that the intersection at each pion mass satisfies the physical pole condition[19] that

$$\left. \frac{d^2}{dp^2} \left[p \cot \delta(p) - (-\sqrt{-p^2}) \right] \right|_{p^2 = -p_{\text{BS}}^2} < 0, \quad (11)$$

where p_{BS} corresponds to a magnitude of the bound state momentum. We also calculate the binding energy solving the Schrödinger equation directly by the Gaussian Expansion Method (GEM)[20], and results represented by thick lines along the bound state condition (blue curve) agree with ones by $p \cot \delta(p)$, as seen in Fig. 3.

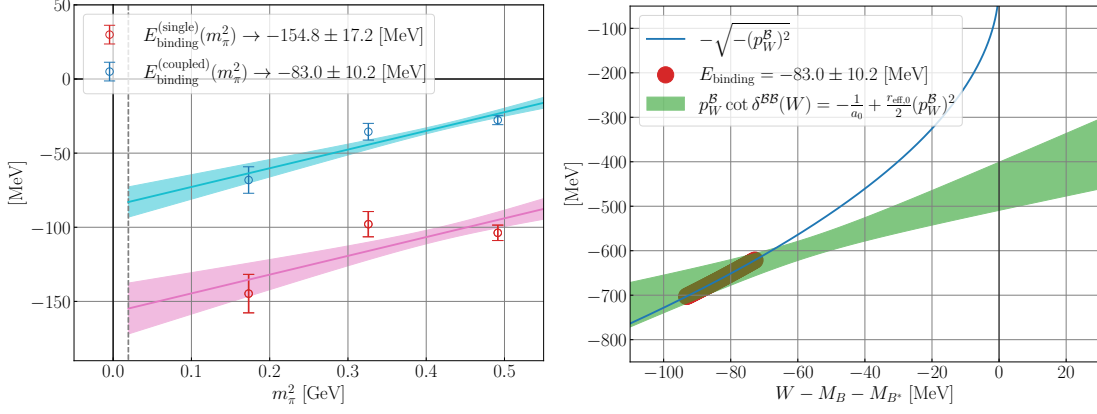


Figure 4: (Left) The binding energy obtained by the GEM as a function of the pion mass squared m_π^2 , together with a linear chiral extrapolation in m_π^2 to $m_\pi = 140$ MeV by solid lines. Results from the single channel analysis (magenta circles) and the coupled channel analysis (cyan circles) are shown. (Right) The ERE at $m_\pi = 140$ MeV (green band), obtained with a_0 and $r_{\text{eff},0}$ by linear extrapolations in m_π^2 , together with the bound state condition, $-\sqrt{-p^2}$ (blue solid curve). An intersection between the two satisfies the physical pole condition and, moreover, agrees well with the binding energy by the GEM at $m_\pi = 140$ MeV (red thick curve along $-\sqrt{-p^2}$).

Fig. 4 (Left) shows the binding energy by the GEM as a function of m_π^2 from the coupled channel analysis (cyan circles), together with a chiral extrapolation linear in m_π^2 by a blue solid. For a comparison, the result from the standard single channel analysis, where the potential in Fig. 1 is used, for example, is also given by magenta circles. At the physical pion mass, $m_\pi = 140$ MeV, we obtain

$$E_{\text{binding}}^{\text{(single,phys)}} = -154.8 \pm 17.2 \text{ MeV}, \quad E_{\text{binding}}^{\text{(coupled,phys)}} = -83.0 \pm 10.2 \text{ MeV}, \quad (12)$$

which shows roughly a 50 % reduction of the binding energy due to contributions from virtual B^* states. Thus the coupled channel analysis is indeed important to estimate the binding energy for T_{bb} more precisely.

As a cross check, we have performed the chiral extrapolation of the effective range expansion (ERE) parameters a_0 and $r_{\text{eff},0}$, obtained from a linear fit in p^2 as $p \cot \delta(p) = -\frac{1}{a_0} + \frac{r_{\text{eff},0}}{2} p^2$ at each pion mass. A linear extrapolation in m_π^2 leads to $a_0 = 0.43(5)$ fm and $r_{\text{eff},0} = 0.18(6)$ fm at $m_\pi = 140$ MeV in the coupled channel analysis. Then the binding energy at the physical point ($m_\pi = 140$ MeV) is alternatively estimated from an intersection between the ERE with these a_0 and $r_{\text{eff},0}$ (green band) and the bound state condition $-\sqrt{-p^2}$ (blue solid curve), as shown in Fig. 4 (Right). The intersection satisfies the physical pole condition and agrees well with the binding energy by the GEM directly extrapolated to the physical point. This agreement in the binding energy between two extrapolations to the physical point provides a validity of our analysis.

4. Conclusion

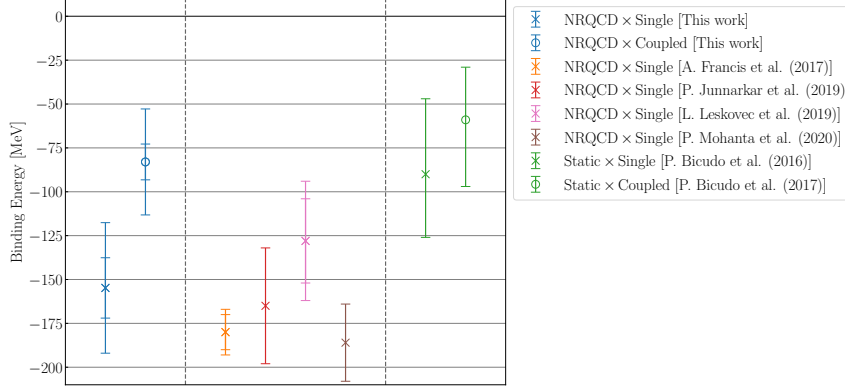


Figure 5: A comparison of binding energies for the tetra quark bound state T_{bb} among several lattice QCD calculations, our results (blue), spectra with the NRQCD (orange, red, magenta and brown), and the static quark potential (green), from single channel (crosses) and couple channel (circles) analyses.

We have calculated S -wave channel potentials between \bar{B} and \bar{B}^* , and found one bound T_{bb} state at three pion masses. The linear chiral extrapolation of the binding energy in m_π^2 gives (12), and adding an empirical systematic error of ± 20 MeV to each value, we compare our results with other lattice results in Fig. 5. First of all we observe a consistency in the binding energy of T_{bb} among the single channel analysis with the NRQCD for b quarks including our results. Secondly the binding energy of T_{bb} increases if the treatment of the b quark on the lattice is changed from the static quark to the NRQCD. Thirdly an inclusion of virtual \mathcal{B}^* effects reduce the binding energy of T_{bb} . In particular, the reduction becomes 50% using the HAL QCD potential combined with the NRQCD for b quarks.

Our numerical calculation has been performed on Yukawa-21 at YITP, Kyoto University. This work is supported in part by the JSPS Grant-in-Aid for Scientific Research (Nos. JP16H03978, JP18H05236).

References

- [1] R. Aaij *et al.* [LHCb], Nature Commun. **13** (2022) no.1, 3351 doi:10.1038/s41467-022-30206-w [arXiv:2109.01056 [hep-ex]].
- [2] A. L. Guerrieri, M. Papinutto, A. Pilloni, A. D. Polosa and N. Tantalo, PoS LATTICE2014 (2015), 106 doi:10.22323/1.214.0106 [arXiv:1411.2247 [hep-lat]].
- [3] Y. Ikeda, B. Charron, S. Aoki, T. Doi, T. Hatsuda, T. Inoue, N. Ishii, K. Murano, H. Nemura and K. Sasaki, Phys. Lett. B **729** (2014), 85-90 doi:10.1016/j.physletb.2014.01.002 [arXiv:1311.6214 [hep-lat]].
- [4] M. Padmanath and S. Prelovsek, Phys. Rev. Lett. **129** (2022) no.3, 032002 doi:10.1103/PhysRevLett.129.032002 [arXiv:2202.10110 [hep-lat]].

- [5] P. Bicudo, K. Cichy, A. Peters and M. Wagner, Phys. Rev. D **93** (2016) no.3, 034501 doi:10.1103/PhysRevD.93.034501 [arXiv:1510.03441 [hep-lat]].
- [6] P. Bicudo, J. Scheunert and M. Wagner, Phys. Rev. D **95** (2017) no.3, 034502 doi:10.1103/PhysRevD.95.034502 [arXiv:1612.02758 [hep-lat]].
- [7] P. Junnarkar, N. Mathur and M. Padmanath, Phys. Rev. D **99** (2019) no.3, 034507 doi:10.1103/PhysRevD.99.034507 [arXiv:1810.12285 [hep-lat]].
- [8] L. Leskovec, S. Meinel, M. Pflaumer and M. Wagner, Phys. Rev. D **100** (2019) no.1, 014503 doi:10.1103/PhysRevD.100.014503 [arXiv:1904.04197 [hep-lat]].
- [9] P. Mohanta and S. Basak, Phys. Rev. D **102** (2020) no.9, 094516 doi:10.1103/PhysRevD.102.094516 [arXiv:2008.11146 [hep-lat]].
- [10] N. Ishii, S. Aoki and T. Hatsuda, Phys. Rev. Lett. **99** (2007), 022001 doi:10.1103/PhysRevLett.99.022001 [arXiv:nucl-th/0611096 [nucl-th]].
- [11] S. Aoki, T. Hatsuda and N. Ishii, Prog. Theor. Phys. **123** (2010), 89-128 doi:10.1143/PTP.123.89 [arXiv:0909.5585 [hep-lat]].
- [12] S. Aoki *et al.* [HAL QCD], PTEP **2012** (2012), 01A105 doi:10.1093/ptep/pts010 [arXiv:1206.5088 [hep-lat]].
- [13] N. Ishii *et al.* [HAL QCD], Phys. Lett. B **712** (2012), 437-441 doi:10.1016/j.physletb.2012.04.076 [arXiv:1203.3642 [hep-lat]].
- [14] S. Aoki *et al.* [HAL QCD], Proc. Japan Acad. B **87** (2011), 509-517 doi:10.2183/pjab.87.509 [arXiv:1106.2281 [hep-lat]].
- [15] B. A. Thacker and G. P. Lepage, Phys. Rev. D **43** (1991), 196-208 doi:10.1103/PhysRevD.43.196
- [16] G. P. Lepage, L. Magnea, C. Nakhleh, U. Magnea and K. Hornbostel, Phys. Rev. D **46** (1992), 4052-4067 doi:10.1103/PhysRevD.46.4052 [arXiv:hep-lat/9205007 [hep-lat]].
- [17] K. I. Ishikawa, H. Matsufuru, T. Onogi, N. Yamada and S. Hashimoto, Phys. Rev. D **56** (1997), 7028-7038 doi:10.1103/PhysRevD.56.7028 [arXiv:hep-lat/9706008 [hep-lat]].
- [18] S. Aoki *et al.* [PACS-CS], Phys. Rev. D **79** (2009), 034503 doi:10.1103/PhysRevD.79.034503 [arXiv:0807.1661 [hep-lat]].
- [19] T. Iritani, S. Aoki, T. Doi, T. Hatsuda, Y. Ikeda, T. Inoue, N. Ishii, H. Nemura and K. Sasaki, Phys. Rev. D **96** (2017) no.3, 034521 doi:10.1103/PhysRevD.96.034521 [arXiv:1703.07210 [hep-lat]].
- [20] M. Kamimura, Phys. Rev. A **38** (1988), 621-624 doi:10.1103/PhysRevA.38.621